Stimulation of Interferon-Stimulated Gene 20 by Thyroid Hormone Enhances Angiogenesis in Liver Cancer

CrossMark

Syuan-Ling Lin[*], Sheng-Ming Wu[†,‡], I-Hsiao Chung[*], Yang-Hsiang Lin[*], Ching-Ying Chen[*], Hsiang-Cheng Chi[*,§], Tzu-Kang Lin[§], Chau-Ting Yeh[¶] and Kwang-Huei Lin[*,¶,#]

[*]Department of Biochemistry, School of Medicine, Chang-Gung University, Taoyuan, Taiwan; [†]Division of Pulmonary Medicine, Department of Internal Medicine, Shuang Ho Hospital, Taipei Medical University, New Taipei City, Taiwan; [‡]Division of Pulmonary Medicine, Department of Internal Medicine, School of Medicine, College of Medicine, Taipei Medical University, Taipei, Taiwan; [§]Radiation Biology Research Center, Institute for Radiological Research, Chang Gung University/Chang Gung Memorial Hospital, Linkou, Taoyuan, Taiwan; [¶]Liver Research Center, Chang Gung Memorial Hospital, Linkou, Taoyuan, Taiwan; [#]Research Center for Chinese Herbal Medicine, College of Human Ecology, Chang Gung University of Science and Technology, Taoyuan, Taiwan

Abstract

Thyroid hormone, 3,3′,5-triiodo-L-thyronine (T_3), mediates several physiological processes, including embryonic development, cellular differentiation and cell proliferation, via binding to its nuclear thyroid receptors (TR). Previous microarray and Chromatin immunoprecipitation (ChIP)-on-ChIP analyses have revealed that interferon-stimulated gene 20 kDa (ISG20), an exoribonuclease involved in the antiviral function of interferon, is up-regulated by T_3 in HepG2-TR cells. However, the underlying mechanisms of ISG20 action in tumor progression remain unknown to date. Here, we verified induction of ISG20 mRNA and protein expression by T_3 in HepG2-TR cells. Based on the ChIP-on-ChIP database, potential thyroid hormone responsive element of the ISG20 promoter region was predicted, and the result confirmed with the ChIP assay. Functional assays showed that forced expression of ISG20 leads to significant promotion of metastasis and angiogenesis, both *in vitro* and *in vivo*. Furthermore, the angiogenic-related protein, interleukin-8 (IL-8), was up-regulated through a T_3-mediated increase in ISG20, as determined using a human angiogenesis array kit. Induction of IL-8 signaling activated the p-JAK2/p-STAT3 pathway, in turn, leading to promotion of tumor metastasis and angiogenesis. Furthermore, ISG20 overexpression in hepatocellular carcinoma (HCC) specimens was positively correlated with clinical parameters, including vascular invasion, α-fetoprotein and tumor size. Higher ISG20 expression was significantly correlated with poorer recurrence-free survival in HCC patients. Our results collectively indicate higher TR-dependent expression of ISG20 in a subset of HCC, supporting an oncogenic role in HCC progression.

Neoplasia (2018) 20, 57–68

Introduction

The thyroid hormone (3,3′,5-triiodo-L-thyronin, T_3), is a central mediator of many physiological processes, including embryonic development, cellular differentiation, metabolism, and regulation of cell growth [1]. These T_3-regulated cellular processes are mediated via a genomic effect, requiring the activation of nuclear thyroid hormone receptors (TRs). Two major TR isoforms, TRα1 and TRβ1 have been identified, which are encoded on human chromosomes 17 and 3, respectively, and expressed differently in developing and adult tissues [2]. Tumor formation is usually caused by tumor cell growth and metastasis, depending on the capacity of tumor cells to recruit their own blood supply. Angiogenesis is essential for human cancer development [3]. The angiogenic process is balanced by the positive regulator, vascular endothelial growth factor (VEGF) [4–7] and the negative regulator, thrombospondin-1 (TSP-1) [8–10]. Previous studies have shown that thyroid hormone induces sprouting angiogenesis through the PDGF-Akt pathway in hypothyroid mice [11] and increases the activity of angiotensin II that supports neovascularization and stimulates endothelial cell motility [12]. Abundance evidence has demonstrated that thyroid status and disease affect tumor formation, growth and metastasis in experimental animals and humans [1]. The collective findings clearly indicate that the thyroid hormone and its receptor play tumor-promoting roles, although the underlying mechanisms of thyroid hormone-stimulated tumor angiogenesis remain to be established.

The interferon-stimulated gene product of 20 kDa, ISG20, has been identified from oligo microarray and ChIP-on-ChIP analyses. We examined the function of ISG20 involved in angiogenesis using MetaCore pathway analysis. ISG20 is a member of the 3′ to 5′ exonuclease superfamily that includes RNases with specificity for single-stranded RNA, and to a lesser extent, DNA [13–15], that possesses antiviral activity. Previous studies suggest that ISG20 participates in the cellular response to virus infection, and its antiviral activity is induced by NF-κB and IRF1 activation [16]. Furthermore, ISG20 promotes angiogenesis [17], although the underlying mechanism is unclear at present. In the current study, we focused on the mechanism underlying the angiogenesis-promoting activity of ISG20 stimulated by thyroid hormone in liver cancer.

Materials and Methods

Cell Culture and Preparation of T₃-Depleted Medium

The human hepatoma cell lines, HepG2 and SK-Hep1 were purchased from the American Type Culture Collection (Taipei, Taiwan). J7 cell line was obtained from Taiwan Hospital. These cells were authenticated by the Mission Biotech using the Promega StemElite™ ID system (Taiwan). These cells were routinely grown in DMEM supplemented with 10% fetal bovine serum. The HepG2 cell line used in this study was stably transfected with TRα (HepG2-TRα1) or TRβ (HepG2-TRβ1), with HepG2-neo as the control cell line. Serum was depleted of T_3 (Td) using resin [18]. Cells were cultured at 37°C in a humidified atmosphere of 95% air and 5% CO_2.

Establishment of ISG20-Overexpressing Cells and Determination of the Effects of IL-8 Depletion Using the Lentiviral System

Human IL-8 shRNA was purchased from the RNAi core center (Academia Sinica, Taiwan). IL-8 shRNA and ISG20 plasmid were cloned into the expression vector pLKO1. The plasmid and lentiviral packaging constructs, pCMV-ΔR8.91 and pMD.G, were cotrans-fected in Her-293T cells via TurboFect reagent Kit (Fermentas Life science, Waltham, MA). After 24-48 h, viral particles with ISG20 were collected to infect SK-Hep1, and viral particles with shIL-8 used to infect the SK-Hep1-ISG20-overexpressing cell line. After 48 h of incubation, cells were transferred to medium containing puromycin for selection.

Quantitative RT-PCR

HepG2-TRα1 and HepG2-TRβ1 cells were seeded into 10 cm diameter dishes and exposed to various treatments for the indicated times, prior to harvesting for RNA extraction. Total RNA was purified using TRIzol reagent (Life Technologies Inc., Carlsbad, CA) according to the supplier's protocol, and cDNA synthesized using a SuperscriptII kit (Life Technologies, Karlsruhe, Germany). Real-time PCR was conducted in 15 μl reaction mixtures containing 25 nM forward and reverse primers and 1×SYBR Green reaction mix (Applied Biosystems, Carlsbad, CA). All reactions were conducted in an ABI PRISM 7500 sequencer (Applied Biosystems, Foster City, CA).

Immunoblotting Analysis

Total cell lysates were analyzed via 8% to 10% (w/v) SDS-PAGE, and the separated proteins transferred to PVDF membranes. After washing in PBST (PBS containing 0.05% [v/v] Tween-20), blots were incubated in blocking solution (PBST with 5% [w/v] skimmed milk powder) containing primary antibody against ISG20, p-JAK2, JAK2 (GeneTex Inc., Irvine, CA), IL-8 (R&D Systems Inc., Minneapolis, MN), p-STAT3(Y705), STAT3 (Cell Signaling Technology Inc., Danvers, MA), VEGF-A, MMP-9, fascin or actin (Santa Cruz Biotechnology Inc., Dallas, TX) at 4°C overnight. After thorough washing, blots were further incubated with HRP-conjugated secondary antibody dissolved in blocking solution. Signals were detected via chemiluminescence using an ECL kit (Amersham) and recorded on X-ray film. JAK2 inhibitor and STAT3 inhibitor (S31-201) were from EMD Millipore (Darmstadt, Germany) and Merck (Canada).

Chromatin Immunoprecipitation (ChIP) Assay

HepG2-TRα1 cells treated with 10 nM T_3 for 24 h or left untreated were harvested and cross-linked with 1% formaldehyde for 10 min at room temperature in DMEM. Reactions were terminated with the addition of 0.125 M glycine. Subsequently, cell lysates were washed three times with PBS and resuspended in lysis buffer (150 mM NaCl, 5 mM EDTA, 50 mM Tris (pH 8.0), 0.1% SDS and 0.1% sodium deoxycholate) containing three protease inhibitors (1 mM PMSF, aprotinin, and leupeptin). Cell lysates were sonicated with a Misonix Sonicator 3000 Homogenizer (Mandel Scientific Company Inc., Guelph, ON, Canada) to disrupt chromatin. Sonicated DNA was between 200 and 1000 bp in length. Products were precleared with 60 μl protein A/G agarose (Sigma Chemicals, St. Louis, MO) for 2 h at 4°C. Complexes were immunoprecipitated with anti-TR and anti-IgG antibodies (R&D Systems, Inc., Minneapolis, MN). Enriched targets were hybridized to promoter microarrays (Welgene Biotech, ChIP-on-chip microarray) spanning –8 kb to +2 kb of the transcription start site (TSS) of 35 000 genes. The promoter fragments of target gene containing the TRE region were detected via q-RT-PCR.

Human Angiogenesis Array Kit

Cell culture supernatant was collected from ISG20-overexpressing and control of SK-Hep1 for 24 h. The angiogenic factors secreted in supernatant was measured using angiogenesis array kit (R&D systems, Minneapolis, MN), according to the manufacturer's instructions. After

thorough washing, blots were further incubated with HRP-conjugated secondary antibody dissolved in blocking solution. Signals were detected via Chemi Reagent Mix and recorded on X-ray film.

ELISA for IL-8

Cell culture supernatant was collected from ISG20-overexpressing stable HCCs or cells treated with IL-8 neutralizing antibody for 24 h. IL-8 secreted in the supernatant was measured using the IL-8 ELISA kit (BioLegend, San Diego, CA), according to the manufacturer's instructions. Absorbance was read at 450 nm using a microplate reader, and concentrations of IL-8 calculated according to the standard curve generated.

In Vitro Tube Formation Assay

Matrigel (Corning Inc., Tewksbury, MA) was dissolved at 4°C. Aliquots (100 µl/well) were added to 48-well plates, which were incubated at 37°C overnight. HUVEC cells were resuspended at a concentration of $3x10^4/100$ µl in conditional medium, and 30-50 µg conditional medium of SK-Hep1-, J7-control or -ISG20- overexpressing cells added to each well of a 48-well plate. After 18-20 h of incubation at 37°C, cell capillary-like structure formation of HUVECs was assessed via microscopy and images of each well obtained under a light microscope. The number of tube branches was calculated using MacBiophotonics Image J software.

In Vivo Matrigel Plug Assay

The matrigel plug angiogenesis assay was adapted from a previously described protocol [5]. Briefly, four week-old male nude mice were randomized into two groups. Specifically, (1) SK-Hep1- and J7-control, and (2) SK-Hep1- and J7-ISG20- overexpressing cell lines were resuspended at a concentration of $5x10^5/50$ µl cells with Matrigel, and 150 µl aliquots were subcutaneously injected into mice. After 7-14 days, plugs were harvested and the hemoglobin content determined using Drabkin's reagent. The remaining plugs were fixed with 4% formaldehyde, embedded in paraffin, and subsequently processed for immunohistochemistry (IHC) staining for the endothelial marker CD31.

In Vivo Chick Chorioallantoic Membrane (CAM) Assay

Angiogenic activity was evaluated using the CAM assay, as described previously [5]. Briefly, fertilized chicken eggs (3 eggs/group) were incubated at 37°C in an 80% humidified atmosphere. On developmental day 8, SK-Hep1-control and SK-Hep1-ISG20-overexpressing cells were resuspended at a density of $2×10^5$ cells/100 µl in Matrigel and placed onto one egg of chick embryo for 4 days. CAMs were subsequently examined via microscopy and photographed. Angiogenesis was quantified by counting the number of blood vessel branches using MacBiophotonics Image J software.

Human HCC Specimens

Biopsies of 220 patients diagnosed with HCC were selected for study after informed consent was obtained. All HCC tissue samples and paired adjacent non-tumor liver tissue specimens were obtained by the Chang Gung Memorial Hospital Medical Research Center (IRB103-4866B), and subjected to western blot and q-RT-PCR analyses.

Statistical Analysis

Results are presented as mean values ± SD of three independent experiments. Statistical analysis was performed in SPSS version 15 (SPSS Inc., Chicago, IL) using the Mann-Whitney test for two groups and one-way ANOVA, followed by Tukey post-hoc test for two or more groups. Kaplan–Meier survival curves were used to analyze survival outcomes. Recurrence-free survival (RFS) with death as an event was analyzed using the log-rank test. P values <0.05 were considered significant.

Results

T_3 Positively Regulates ISG20 mRNA and Protein Levels in HCC Cells

We employed oligo-microarray and ChIP-on-ChIP analyses to identify the genes directly regulated by T_3 in HepG2-TRα1 cells. The major pathway of TR-binding genes is a set of new blood vessel formation by MetaCore pathway analysis. The top of TR-binding/-regulated gene is ISG20 [19]. However, its function in angiogenesis is currently unclear. To validate the regulation of ISG20 by T_3, we used isogenic HepG2 cell lines stably expressing wild-type TRα1 (HepG2-TRα1) and TRβ1 (HepG2-TRβ1). Cells transfected with empty vector were used as a negative control (HepG2-Neo). Notably, the ISG20 mRNA and protein levels of HepG2-TRα1 and HepG2-TRβ1 cells were enhanced following T_3 treatment in a time- and dose-dependent manner (Figure 1, A and B). Protein expression of ISG20 was additionally determined in SK-Hep1 cells expressing low levels of endogenous TR treated without or with T_3 for 12-48 h. The ISG20 protein level was marginally increased in SK-Hep1 cells treated with T_3 (Figure 1B). To further determine whether the thyroid hormone response element (TRE) of ISG20 is directly targeted by TR proteins, the chromatin immunoprecipitation (ChIP) assay was performed. TR and RXR bound to ISG20 promoter fragments were pulled down with C4 and RXR antibodies, respectively, but not IgG antibody (Supplementary Figure 1A). GAPDH were used as the negative control. Our results clearly demonstrate that ISG20 is up-regulated by T_3, and TR binds directly to the ISG20 promoter.

Angiogenic Effects of Thyroid Hormone and ISG20 in Hepatoma Cells

Previous studies have suggested that T_3 promotes angiogenesis though the PDGF-Akt pathway [11]. To examine whether T_3 induces angiogenesis in liver cancer, the human umbilical vein endothelial cell (HUVEC) in vitro model was employed. The conditional medium (CM) from HepG2-TRα1 cell lines treated with 10 nM T_3 significantly promoted tube formation in HUVECs (Figure 1C). To further confirm T_3-promoted angiogenesis through ISG20 expression, the CM which was collected from ISG20 depleted- and T_3 (10 nM) treated-HepG2-TRα1cells suppressed tube formation in HUVECs significantly (Figure 1D). The tube formation was also decreased about 3.5-fold in HepG2-TRα1-shISG20 cells compared to that in shControl cells (Figure 1D). To examine the role of ISG20 in tumor progression or angiogenesis, ISG20 overexpression in SK-Hep1 (SK-Hep1-ISG20) and J7 (J7-ISG20) cell lines was established via the lentivirus-based system (Figure 3C). The CM of overexpressing ISG20, but not control CM, dramatically promoted tube formation in HUVECs (Figure 1E). Tube formation was increased about 6- and 2.5-fold in SK-Hep1- and J7-ISG20 cells, respectively, compared to that in control cells (Figure 1E). Our results indicate that ISG20 is up-regulated by T_3, supporting its involvement in thyroid hormone-promoted angiogenesis in hepatoma cells.

Overexpression of ISG20 Significantly Promotes Tumor Angiogenesis In Vivo

To evaluate whether ISG20 promotes HUVEC-primed angiogenesis in vivo, mouse xenograft model Matrigel plug formation or chick
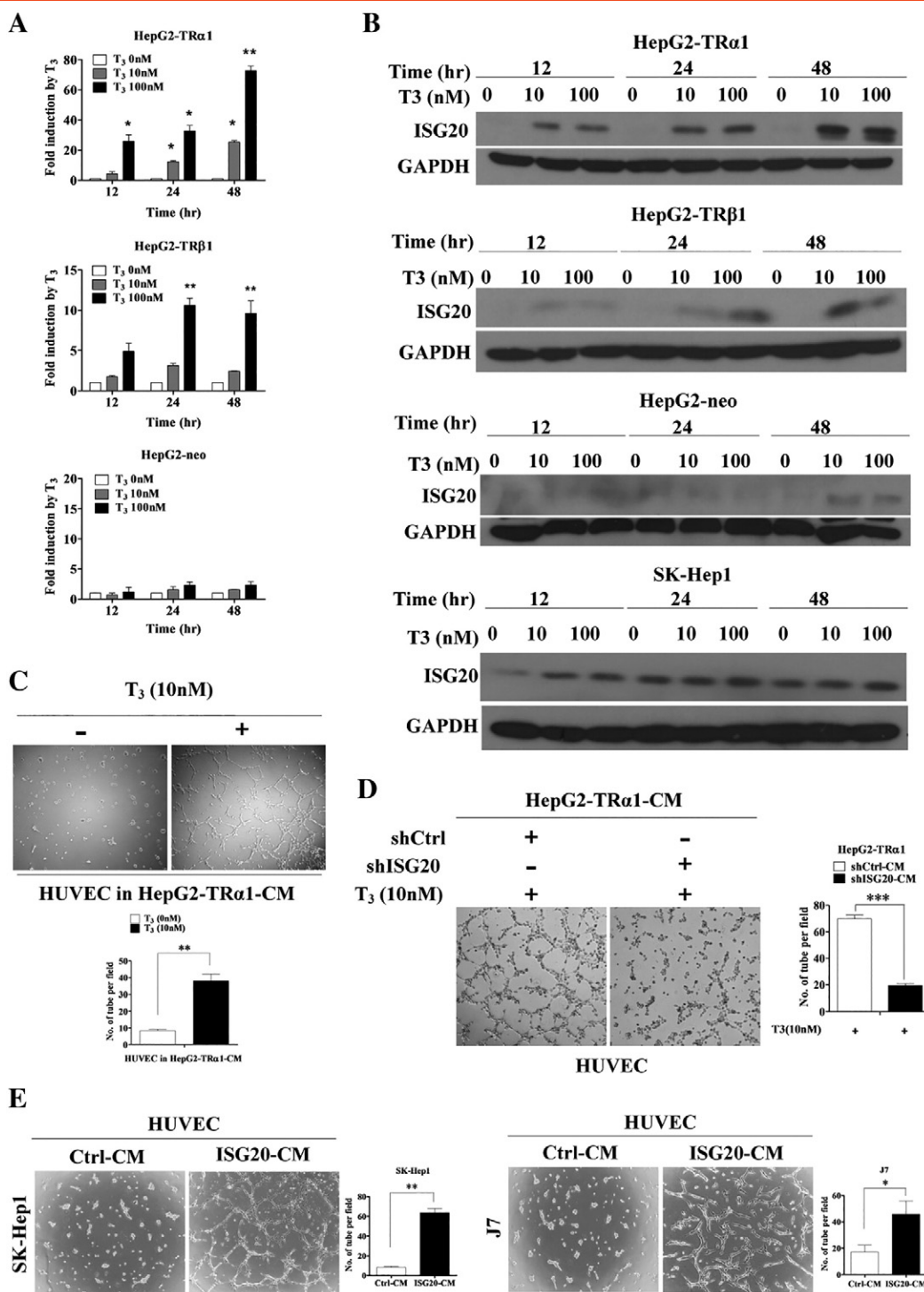
Figure 1. T$_3$ positively regulates mRNA and protein levels of ISG20 and effects of T$_3$ and ISG20 on angiogenesis in hepatoma cells. (A) ISG20 mRNA and (B) protein expression in TR stable cell lines (HepG2-TRα1, HepG2-TRβ1, HepG2-neo control or SK-Hep1) incubated for 12, 24 or 48 h in the absence or presence of T$_3$ (10 or 100 nM). Total RNA or protein was isolated and analyzed via qRT-PCR and western blot, respectively. (C) HepG2-TRα1 cells were incubated with T$_3$ (10 nM) for 24 h, and conditional medium (CM) was collected. HUVECs were incubated with CM for 16 h, and cell capillary-like structure formation was photographed and counted. (D) HepG2-TRα1-shCtrl and HepG2-TRα1-shISG20 cells were incubated with T$_3$ (10 nM) for 24 h, and CMs were collected. HUVECs were incubated with CM for 16 h, and cell capillary-like structure formation was photographed and counted. (E) HUVECs were incubated with CM collected from SK-Hep1- and J7-ISG20 and control cells, and cell capillary-like structure formation in HUVECs was photographed and counted. Data are presented as means ± SD from three independent experiments, each performed in triplicate (*$p < 0.05$; **$p < 0.01$).

embryo CAM assay was conducted. Matrigel mixed with SK-Hep1-ISG20 and J7-ISG20 cells significantly enhanced blood vessel growth. The hemoglobin content of the plug was higher following incubation with ISG20-overexpressing cells, indicating increased hepatoma-related angiogenesis *in vivo* (Figure 2A). Furthermore, SK-Hep1 and J7 cells overexpressing ISG20 induced
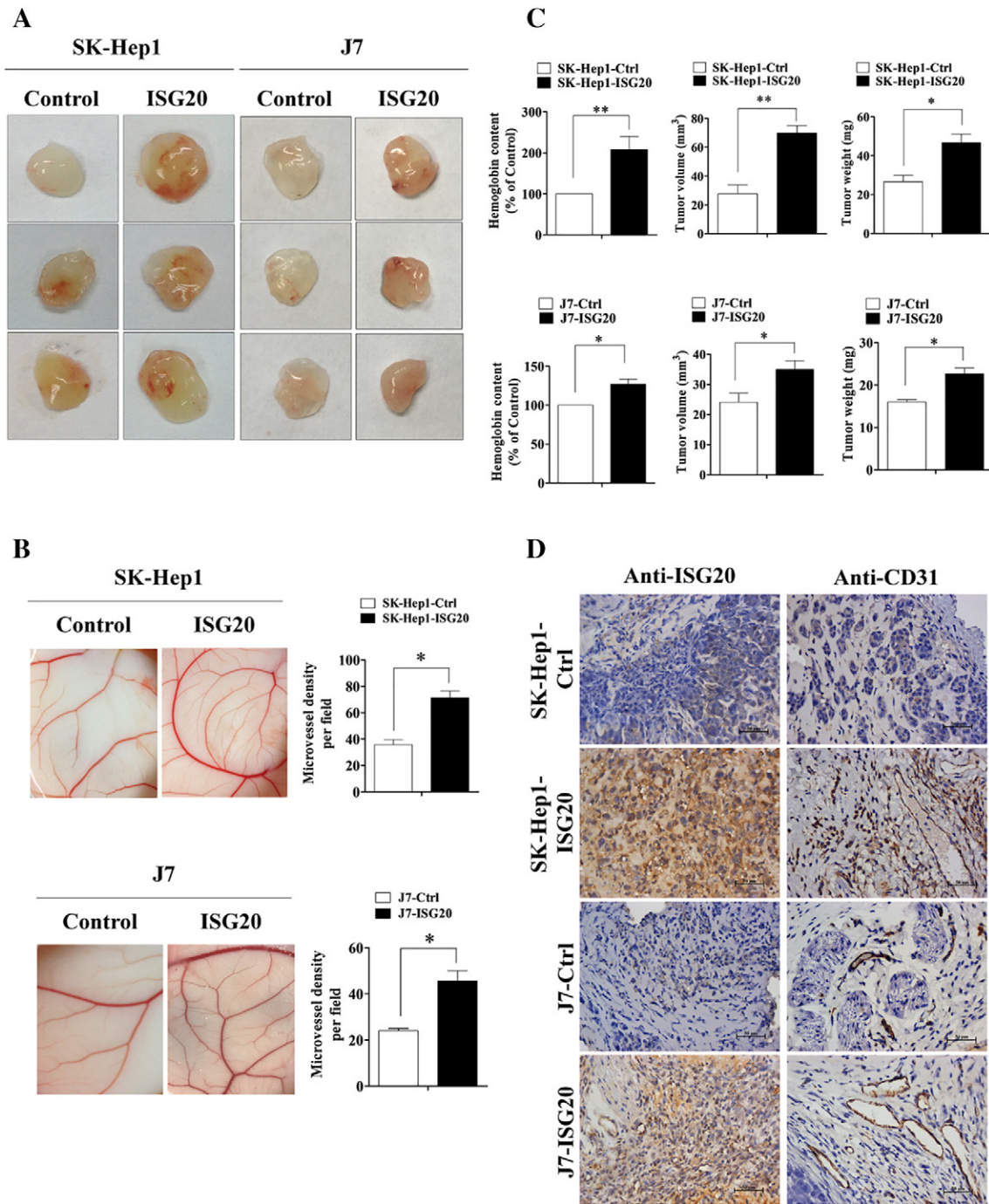
Figure 2. Overexpression of ISG20 significantly promotes tumor angiogenesis *in vivo*. (A) Mice were subcutaneously injected with Matrigel mixed with control or ISG20-overexpressing cells (SK-Hep1 and J7) for 7 days. Plugs excised from mice were photographed (n = 8). (B) ISG20-overexpressing and control cells mixed in Matrigel were placed on chick CAMs, and images of CAM artery branches in groups obtained on developmental day 12 (left panel). Quantification of the microvessel number in the CAM assay (n = 3, right panel). (C) Hemoglobin content in plugs isolated from mice at day 7, measured using Drabkin's procedure. Tumor (plug) volume and weight were measured. (D) Levels of ISG20 and the endothelial marker, CD31, were determined from plugs of ISG20-overexpressing and control cells via IHC staining. Data are presented as means ± SD (*$p < 0.05$; **$p < 0.01$).

significantly enhanced CAM angiogenesis (Figure 2B). The hemoglobin content was additionally positively correlated with tumor growth (Figure 2C). Finally, higher expression of CD31, an endothelial marker, was observed in the ISG20-overexpressing cell line from the *in vivo* Matrigel plug formation assay

(Figure 2D). On the contrary, CM of ISG20-knockdown HepG2-TRα1 cells under T₃ addition (10 nM) reduced CAM angiogenesis (Supplementary Figure 1B). The results clearly suggest that ISG20 functions to promote HUVEC-primed angiogenesis and tumor growth *in vivo*.

IL-8 is a Major Mediator of ISG20-Promoted Tumor Angiogenesis

To identify the angiogenic factors induced by ISG20 in HCC cells, a human angiogenesis array kit [20,21] was screened using CM from the SK-Hep1-Ctrl and SK-Hep1-ISG20 cell lines. Markedly elevated levels of IL-8 and moderate increases in MMP-9, coagulation factor III (TF) and Amphiregulin (AR), well-known pro-angiogenic factors, [22–24] were observed in the SK-Hep1-ISG20 cell line, compared to the control cell line (Figure 3*A*, left panel). Conversely, insulin-like growth factor binding protein-3 (IGFBP-3) and Endostatin (collagen XVIII) levels were reduced upon ISG20 overexpression (Figure 3*A*, left panel). Endostatin is an endogenous inhibitor of angiogenesis and tumor growth while IGFBP-3 is reported to play a dual role in angiogenesis [25,26]. The quantitative result was shown (Figure 3*A*, right panel). In view of its marked elevation, we further investigated
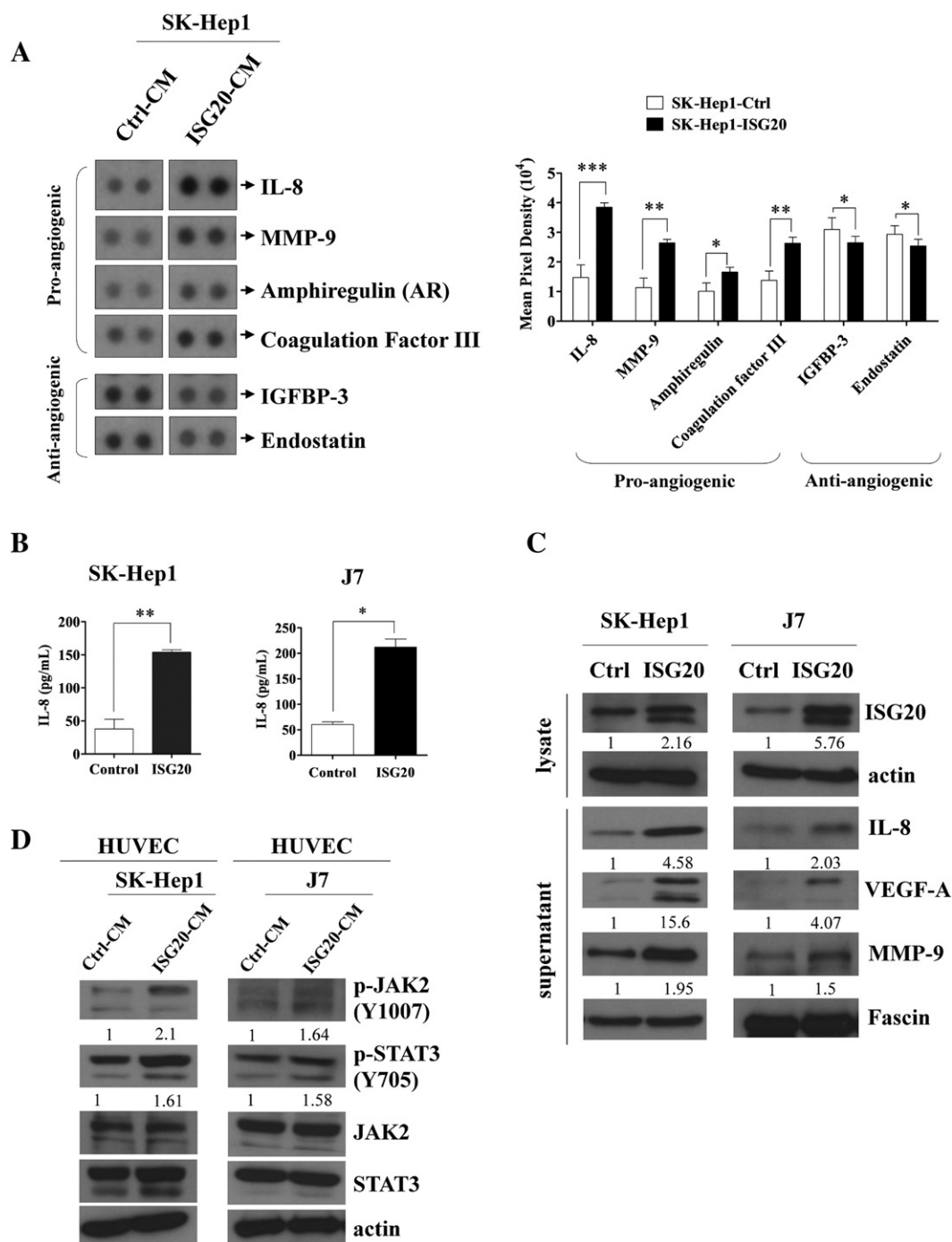

Figure 3. IL-8 is major mediator of ISG20-promoted tumor angiogenesis. (A) Human angiogenesis array membranes were used to analyze secretion of angiogenic growth factors by CM of control and ISG20-overexpressing SK-Hep1 cells (left panel). Quantitative data is shown in the right panel. (B) Determining the tumor expression of the major pro-angiogenic factor, IL-8, in response to ISG20-overexpressing and control SK-Hep1 or J7 cells via ELISA. (C) Western blot analysis of the expression of ISG20 and pro-angiogenic factors, IL-8, VEGF-A and MMP-9, in ISG20-overexpressing or control SK-Hep1 or J7 cells. (D) Expression of p-JAK2 and p-STAT3 in HUVECs incubated with CM of ISG20-overexpressing cells analyzed via western blot. Data are presented as means ± SD (*$p < 0.05$; **$p < 0.01$).

the role of IL-8 in ISG20-stimulated angiogenesis. Induction of IL-8 by ISG20 using CM from cell lines was confirmed via ELISA. The IL-8 level was significantly higher in SK-Hep1- and J7-ISG20 cells, compared to control cells (Figure 3B). Expression of IL-8 protein was dramatically increased by ISG20 overexpressing in HCC stable cell lines. In addition to angiogenic factors, VEGF-A and MMP-9 protein levels were higher in SK-Hep1- and J7-ISG20 cells, as evident from western blot (Figure 3C). Previous studies have shown that tumor-derived IL-8 activates endothelial cells in tumor vasculature and triggers JAK2 and STAT3 activation (p-JAK2/p-STAT3) to promote angiogenesis [27]. Notably, in our experiments, CM from ISG20-overexpressing HCC stable cell lines dramatically activated JAK2/STAT3 phosphorylation in HUVECs (Figure 3D). The data collectively support the theory that IL-8 is an important angiogenic factor that contributes to ISG20-promoted angiogenesis through the p-JAK2/p-STAT3 signaling pathway.

Knockdown of IL-8 Decreases HUVEC-Primed Angiogenesis In Vitro

To evaluate whether IL-8 contributes to HUVEC-primed angiogenesis in the microenvironment of liver cancer, IL-8 shRNA stable cell lines were established. An IL-8 neutralizing antibody blocking IL-8 expression in ISG20-overexpressing HCC stable lines was employed to determine whether reduction of IL-8 inhibits angiogenesis in an *in vitro* tube formation assay. IL-8 expression was greatly repressed by an IL-8 specific shRNA (Figure 4A, left panel) or its specific neutralizing antibody (Figure 4A, right panel) in two cell lines. Depletion of IL-8 by its shRNA (Figure 4B) or neutralizing antibody (Figure 4C) in ISG20-overexpressing HCC stable lines strongly abolished ISG20-promoted tube formation in HUVECs. Quantitative data showed a higher number of tubes in control shRNA than IL-8 shRNA of ISG20-overexpressing stable HCC cell lines (Figure 4B, bottom panel). Similar suppression of ISG20-promoted angiogenesis was observed upon IL-8 depletion (Figure 4C, bottom panel). Additionally, phosphorylation of JAK2 and STAT3 signaling proteins in HUVECs were decreased by CM from ISG20-overexpressing stable HCC lines depleted of IL-8 (Figure 4D). Using JAK2 inhibitor or STAT3 inhibitor (S31-201) also dramatically abolished ISG20-promoted tube formation in HUVECs (Figure 4E). The quantitative data was shown (Figure 4E, bottom panel). Additionally, the phospho-JAK2 and STAT3 signaling proteins in ISG20-overexpressing stable HCC lines were decreased by these inhibitors (Supplementary Figure 2). Taken together, the results suggest that ISG20 promotes angiogenesis through enhancing IL-8 expression and JAK/STAT3 activation *in vitro*.

Suppression of IL-8 Eliminates ISG20-Enhanced Tumor Angiogenesis In Vivo

We additionally investigated whether suppression of IL-8 affects ISG20-enhanced tumor angiogenesis *in vivo* via the Matrigel plug formation and CAM assay. To this end, IL-8 knockdown in ISG20-overexpressing stable lines and plug formation via subcutaneous injection were achieved. More blood vessels were observed and plug size was bigger in control shRNA than IL-8-depleted of ISG20-overexpression stable cell lines (Figure 5A). Moreover, the hemoglobin content of plugs formed from ISG20-overexpressing cells depleted of IL-8 was decreased (Figure 5A). In the CAM assay, formation of new blood vessels was dramatically decreased following IL-8 knockdown in ISG20-overexpressing stable cells (Figure 5B).

Finally, CD31 expression in the plug of control shRNA cells was higher than that in the plug of the IL-8 depletion group, as observed with IHC staining (Figure 5C). Based on these findings, we propose that ISG20 promotes IL-8 expression to enhance HUVEC-primed angiogenesis *in vivo*.

ISG20 is Highly Expressed in Human HCC and Correlated with IL-8 Expression

We further investigated the role of ISG20 in liver cancer progression and its correlation with IL-8 in clinical specimens. ISG20 mRNA level was overexpressed in 65.9% (145 out of 220) cancerous tissues, compared to matched adjacent tissues (data not shown). ISG20 expression was additionally analyzed in the web-based microarray database, *ONCOMINE*. High levels of ISG20, TRα1 and IL-8 were detected in HCCs, compared to normal tissues, from the Mas microarray database (Figure 6A). Furthermore, expression of ISG20 and TRα was significantly correlated with recurrence-free survival of HCC patients (Figure 6B). Statistical analysis revealed moderate positive relationships between expression of ISG20, TRα (Pearson's $r = 0.394$, $p < 0.005$) and IL-8 (Pearson's $r = 0.334$, $p < 0.005$) in HCCs (Figure 6C). Analysis of the clinicopathological significance of ISG20 and IL-8 expression in 220 paired HCCs revealed that levels of both mRNA were significantly enhanced in relation to vascular invasion ($p < 0.05$), high α-fetoprotein (AFP) concentration (>25 ng/ml, $p < 0.05$), and bigger tumor size (>5cm, $p < 0.05$) (Figure 6D). In addition, the potential function of ISG20 is to inhibit the replication of hepatitis C virus [28]. Thus, we analyzed the relationship between ISG20 expression and HCV infection in HCC specimens. However, the levels of ISG20 didn't correlate with HCV infection (Supplementary Figure 3). Moreover, enhanced TRα and concomitantly elevated ISG20 protein levels were observed in matched cancerous tissues in 20 % cases (10 out of 50; Figure 6E). Based on these results, we conclude that ISG20 expression is higher in HCCs and significantly correlated with IL-8 and TRα.

Discussion

In this study, we focused on characterization of ISG20 identified from oligo microarray screening for T$_3$-responsive genes in HepG2-TRα1 cells. The significance of T$_3$ modulation of ISG20 in HCC has not been established to date. Our results suggest that ISG20 is positively modulated by T$_3$ at both mRNA and protein levels. Data from the ChIP assay revealed that TR proteins directly bind TRE of the ISG20 promoter region. T$_3$ has been shown to induce angiogenesis-related proteins, such as VEFG, bFGF and PDGF [11], leading to promotion of sprouting angiogenesis. In our experiments, CM from T$_3$-treated HepG2-TRα1 enhanced angiogenesis in HUVECs, as observed with the tube formation assay *in vitro*. However, the molecular mechanisms of T$_3$-induced tumor angiogenesis remain unknown.

Recent studies have demonstrated that ISG20 is an interferon (IFN)-induced gene product with Mr 20,000 [29]. ISG20 is a member of the 3′ to 5′ exonuclease family that specifically degrades single-stranded RNA [30] and, to a lesser extent, DNA, suggesting that ISG20 is a mediator of the innate immune response and potentially involved in the antiviral function of IFN against RNA viruses [14,29]. Moreover, IFN exerts antitumor activity against various human malignancies and appears to suppress angiogenesis through preventing endothelial cell differentiation, and not direct antiproliferative effects. Interestingly, a previous report showed that
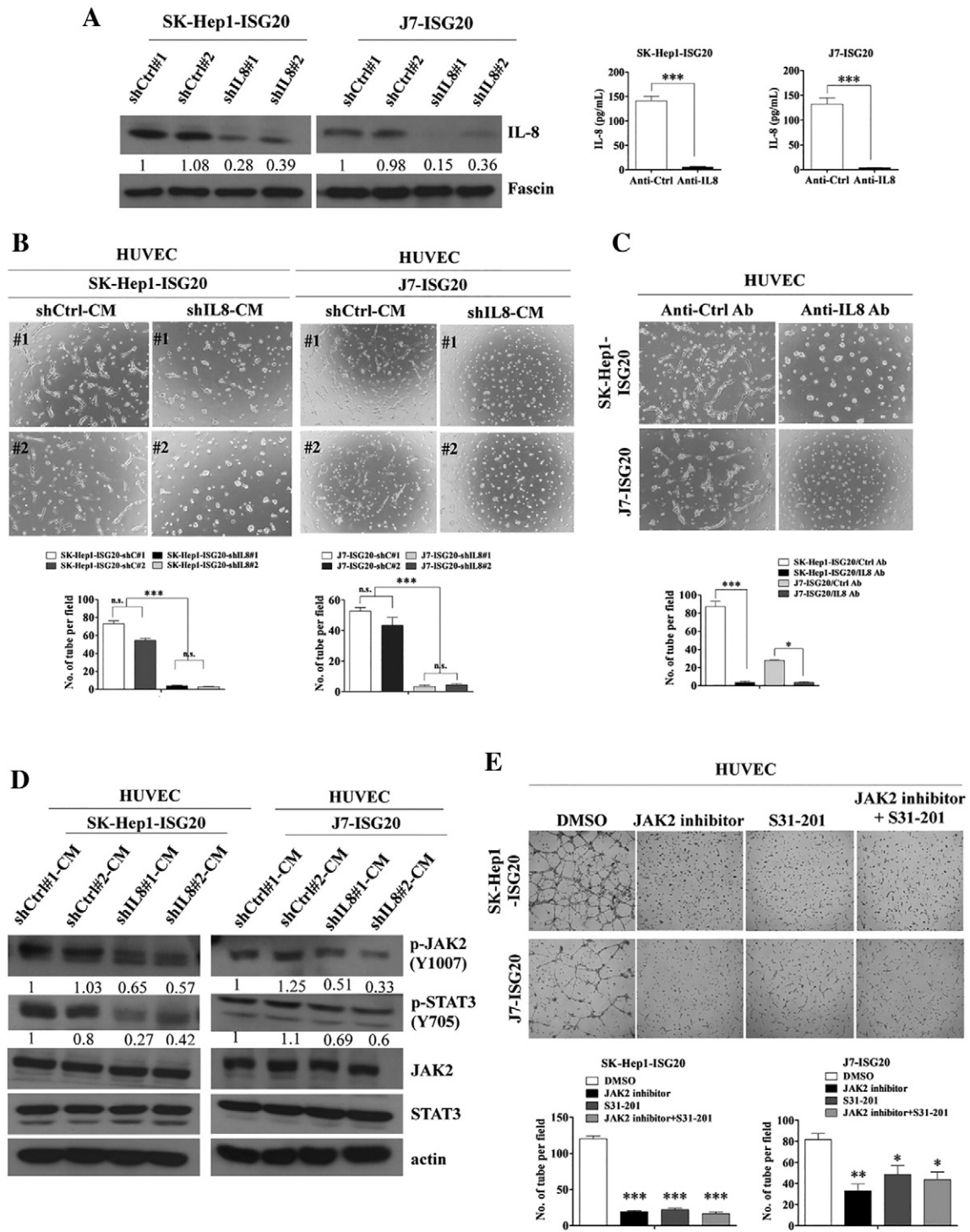
Figure 4. Knockdown of IL-8 decreases HUVEC-primed angiogenesis *in vitro* (A) IL-8 depletion in ISG20-overexpressing cells (SK-Hep1 and J7), observed via western blot (left panel) or in IL-8 neutralizing antibody using ELISA (right panel). (B) CM of IL-8 knockdown or control SK-Hep1- and J7-ISG20 cells was collected, incubated with HUVECs, and cell capillary-like structure formation was photographed and counted. (C) CM of IL-8 neutralizing antibody (0.2 μg/ml) and control antibody-treated SK-Hep1- and J7-ISG20 cells was collected. HUVECs were incubated with CM, and cell capillary-like structure formation was photographed and counted. (D) Western blot analysis of p-JAK2 and p-STAT3 protein expression between HUVECs incubated with CM of IL-8 knockdown and control of ISG20-overexpressing SK-Hep1 or J7 cells. (E) CM of JAK2 inhibitor treated- (100 μM), or S31-201 treated- (100 μM), or DMS0-treated SK-Hep1- or J7-ISG20 cells were collected. HUVECs were incubated with CM, and cell capillary-like structure formation was photographed and counted. Data are presented as means $\pm$ SD (*$p < 0.05$; **$p < 0.01$).

ISG20 expression is induced by IFN but does not inhibit angiogenesis upon overexpression in HUVECs. Furthermore, a dominant-negative mutant (showing loss of exonuclease activity) of ISG20 suppressed tube formation in HUVECs [17] via an unknown mechanism. Here, we obtained evidence showing that ISG20 promotes tumor angiogenesis via regulation of IL-8 in HCC cells. Moreover, our
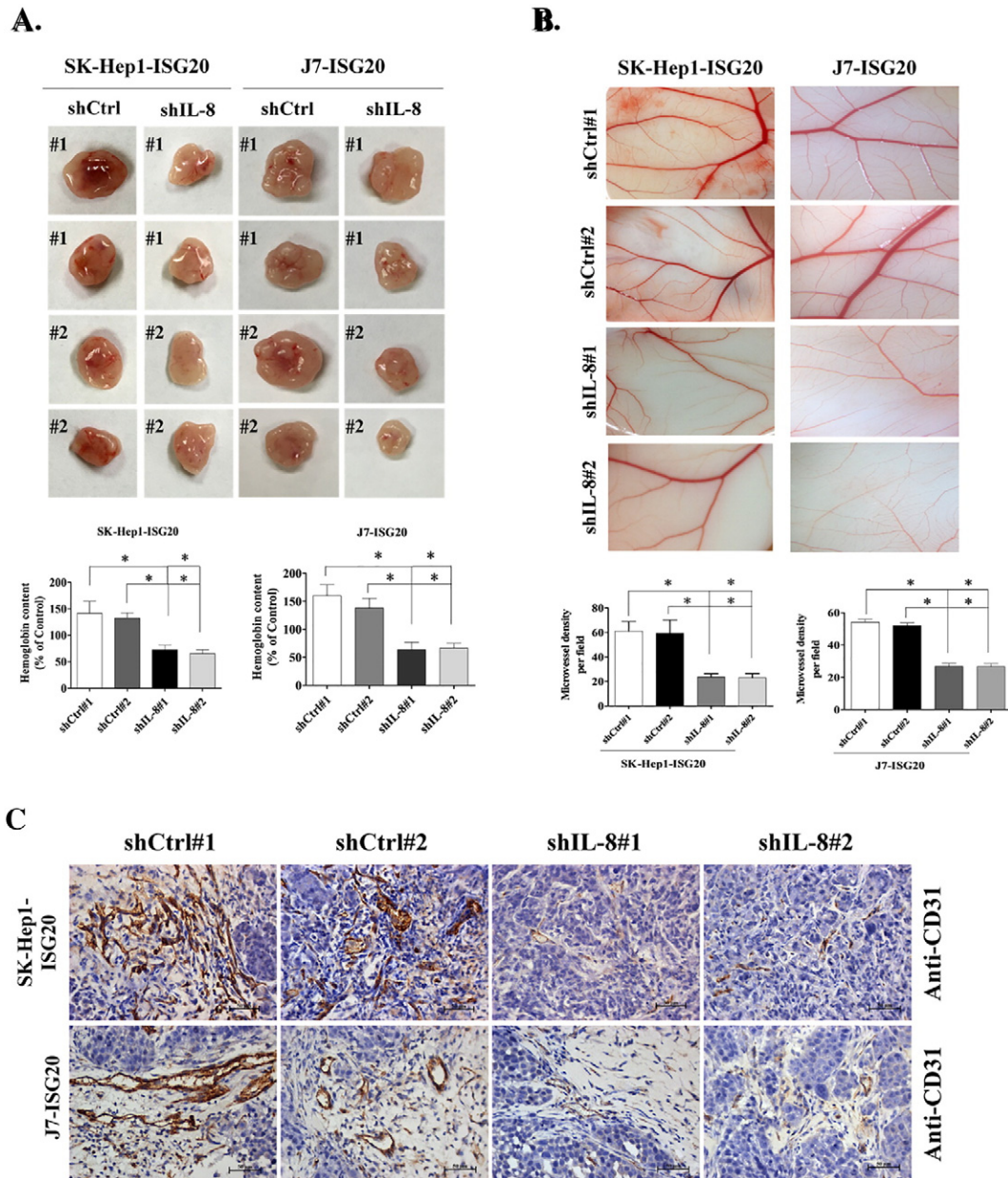
Figure 5. Suppression of IL-8 eliminates ISG20-enhanced tumor angiogenesis *in vivo*. (A) Mice were subcutaneously injected with Matrigel mixed with IL-8 depletion or control vector-containing ISG20-overexpressing cells (SK-Hep1 or J7) for 7 days. Plugs excised from mice were photographed (n = 4) and the hemoglobin content isolated on day 7 was measured using Drabkin's procedure. (B) CM of IL-8 knockdown or control vector-containing ISG20-overexpressing cells mixed in Matrigel were placed on chick CAMs. CAM artery branches in groups were photographed on developmental day 12, and the microvessel number was quantified in the CAM assay (n = 3). (C) Expression of the endothelial marker, CD31, in IL-8 knockdown or control vector-containing ISG20-overexpressing cells was determined from plugs via IHC staining. Data are presented as means ± SD (*$p < 0.05$; **$p < 0.01$).

findings suggest that ISG20 positively regulates IL-8 expression and activates JAK2/STAT3 phosphorylation in hepatoma cells. IL-8 is reported to enhance angiogenesis through multiple signaling pathways, including JAK2/STAT3, Akt, and Erk1/2 cascades [27]. However, we did not observe an association between IL-8 overexpression and increased Akt or Erk1/2 expression and activity. The discrepancy between our findings and those reported previously may be due to cell type specificity. Notably, activation of the CXCR2 receptor by IL-8 leads to JAK2-dependent phosphorylation of a member of the signal transducer and activator of transcription family,

STAT3, which positively mediates angiogenesis in multiple cancers [31,32]. Recently, Dodd et al. [33] reported that STAT3 cooperates with mTOR to enhance angiogenesis. Moreover, endothelial progenitor cells activate the JAK2/STAT3 signaling pathway to accelerate angiogenesis [27].

Thyroid hormone is a critical mediator of diverse cellular functions, including cellular metabolism, proliferation and organ development, in the normal physiological environment [1]. Recent studies have demonstrated nongenomic actions of thyroid hormone-induced angiogenesis mediated by the cell surface receptor integrin αvβ3
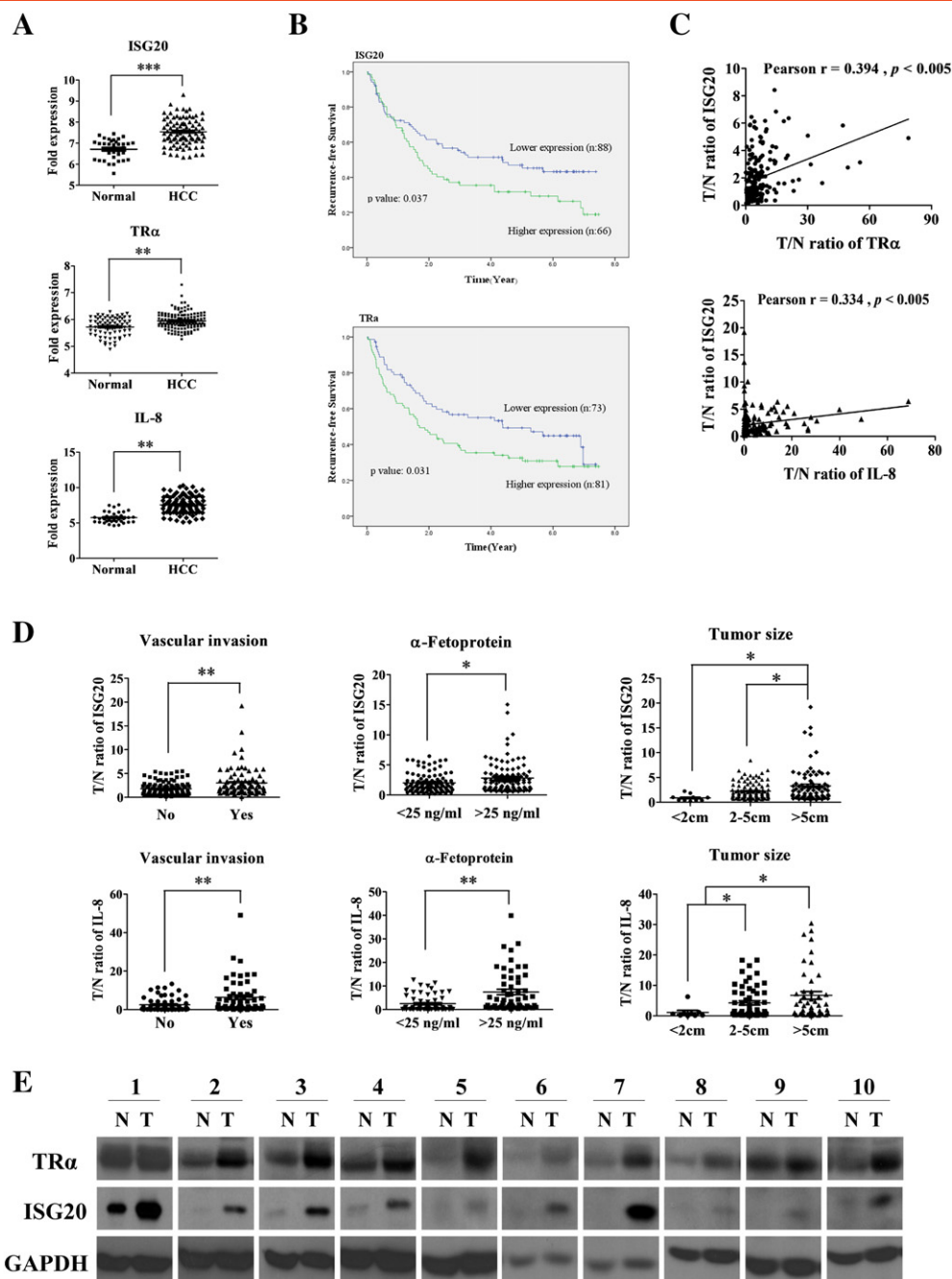
Figure 6. ISG20 is highly expressed in human HCC and positively correlated with IL-8 expression in specimens. (A) ISG20, TRα and IL-8 gene expression analysis using the *ONCOMINE* database. (B) Kaplan-Meier analysis of recurrence-free survival based on ISG20 and TR expression levels in 154 paired HCC specimens. Mean expression levels of these genes were used as the cut-off. (C) Pearson correlation of ISG20, IL-8 and TR were analyzed. (D) q-RT-PCR analysis of ISG20 and IL-8 mRNA expression in 220 HCC specimens. (E) Representative western blot image (10 out of 50 = 20%) of ISG20 and TR protein levels between cancerous and matched adjacent tissues were shown. Data are presented as means ± SD (*$p < 0.05$; **$p < 0.01$).

[34]. Chen et al. [11] reported that T₃ enhances PDGF receptor β protein to induce angiogenesis in hypothyroid heart. However, the importance of TR involvement in angiogenesis has not been reported to date. Overexpression of TR and Wnt pathway activation have been shown to promote colorectal cancer formation [35]. Further evidence has been obtained showing that aberrant and mutant TR play a role in promotion of cancer progression via up-regulation of lipocalin 2 through the MET/FAK signaling pathway to promote HCC metastasis, [36] and repression of microRNA-130b by T₃/TR

enhances cell motility via up-regulation of epithelial-mesenchymal transition (EMT)-related genes, MMP-9, p-mTOR, p-Erk1/2, p-Akt and p-STAT3, in hepatoma cells [37]. In the current study, we showed that ISG20 promotes angiogenesis of hepatoma cell lines *in vitro* and *in vivo*, and is positively correlated with vascular invasion and tumor size in HCC tissues.

In conclusion, we have identified a novel mechanism involving ISG20 induction by T₃ via the IL-8/p-JAK2/p-STAT3 signaling pathway to promote tumor angiogenesis in HCC.

Conflict of Interest

The authors declare no conflicts of interest.

References

[1] Wu SM, Cheng WL, Lin CD, and Lin KH (2013). Thyroid hormone actions in liver cancer. *Cell Mol Life Sci* **70**, 1915–1936.

[2] Munoz A and Bernal J (1997). Biological activities of thyroid hormone receptors. *Eur J Endocrinol* **137**, 433–445.

[3] Baeriswyl V and Christofori G (2009). The angiogenic switch in carcinogenesis. *Semin Cancer Biol* **19**, 329–337.

[4] Herbert SP and Stainier DY (2011). Molecular control of endothelial cell behaviour during blood vessel morphogenesis. *Nat Rev Mol Cell Biol* **12**, 551–564.

[5] Tzeng HE, Chen PC, Lin KW, Lin CY, Tsai CH, Han SM, Teng CL, Hwang WL, Wang SW, and Tang CH (2015). Basic fibroblast growth factor induces VEGF expression in chondrosarcoma cells and subsequently promotes endothelial progenitor cell-primed angiogenesis. *Clin Sci (Lond)* **129**, 147–158.

[6] McColl BK, Stacker SA, and Achen MG (2004). Molecular regulation of the VEGF family – inducers of angiogenesis and lymphangiogenesis. *APMIS* **112**, 463–480.

[7] Lin CY, Hung SY, Chen HT, Tsou HK, Fong YC, Wang SW, and Tang CH (2014). Brain-derived neurotrophic factor increases vascular endothelial growth factor expression and enhances angiogenesis in human chondrosarcoma cells. *Biochem Pharmacol* **91**, 522–533.

[8] Wang JM, Isenberg JS, Billiar TR, and Chen AF (2013). Thrombospondin-1/CD36 pathway contributes to bone marrow-derived angiogenic cell dysfunction in type 1 diabetes via Sonic hedgehog pathway suppression. *Am J Physiol Endocrinol Metab* **305**, E1464-472.

[9] Zhou L, Isenberg JS, Cao Z, and Roberts DD (2006). Type I collagen is a molecular target for inhibition of angiogenesis by endogenous thrombospondin-1. *Oncogene* **25**, 536–545.

[10] Iruela-Arispe ML, Lombardo M, Krutzsch HC, Lawler J, and Roberts DD (1999). Inhibition of angiogenesis by thrombospondin-1 is mediated by 2 independent regions within the type 1 repeats. *Circulation* **100**, 1423–1431.

[11] Chen J, Ortmeier SB, Savinova OV, Nareddy VB, Beyer AJ, Wang D, and Gerdes AM (2012). Thyroid hormone induces sprouting angiogenesis in adult heart of hypothyroid mice through the PDGF-Akt pathway. *J Cell Mol Med* **16**, 2726–2735.

[12] Mousa SA, Lin HY, Tang HY, Hercbergs A, Luidens MK, and Davis PJ (2014). Modulation of angiogenesis by thyroid hormone and hormone analogues: implications for cancer management. *Angiogenesis* **17**, 463–469.

[13] Espert L, Degols G, Gongora C, Blondel D, Williams BR, Silverman RH, and Mechti N (2003). ISG20, a new interferon-induced RNase specific for single-stranded RNA, defines an alternative antiviral pathway against RNA genomic viruses. *J Biol Chem* **278**, 16151–16158.

[14] Espert L, Degols G, Lin YL, Vincent T, Benkirane M, and Mechti N (2005). Interferon-induced exonuclease ISG20 exhibits an antiviral activity against human immunodeficiency virus type 1. *J Gen Virol* **86**, 2221–2229.

[15] Nguyen LH, Espert L, Mechti N, and Wilson III DM (2001). The human interferon- and estrogen-regulated ISG20/HEM45 gene product degrades single-stranded RNA and DNA in vitro. *Biochemistry* **40**, 7174–7179.

[16] Espert L, Rey C, Gonzalez L, Degols G, Chelbi-Alix MK, Mechti N, and Gongora C (2004). The exonuclease ISG20 is directly induced by synthetic dsRNA via NF-kappaB and IRF1 activation. *Oncogene* **23**, 4636–4640.

[17] Taylor KL, Leaman DW, Grane R, Mechti N, Borden EC, and Lindner DJ (2008). Identification of interferon-beta-stimulated genes that inhibit angiogenesis in vitro. *J Interf Cytokine Res* **28**, 733–740.

[18] Samuels HH, Stanley F, and Casanova J (1979). Depletion of L-3,5,3′-triiodothyronine and L-thyroxine in euthyroid calf serum for use in cell culture studies of the action of thyroid hormone. *Endocrinology* **105**, 80–85.

[19] Chung IH, Liu H, Lin YH, Chi HC, Huang YH, Yang CC, Yeh CT, Tan BC, and Lin KH (2016). ChIP-on-chip analysis of thyroid hormone-regulated genes and their physiological significance. *Oncotarget* **7**, 22448–22459.

[20] Abuhusain HJ, Matin A, Qiao Q, Shen H, Kain N, Day BW, Stringer BW, Daniels B, Laaksonen MA, and Teo C, et al (2013). A metabolic shift favoring sphingosine 1-phosphate at the expense of ceramide controls glioblastoma angiogenesis. *J Biol Chem* **288**, 37355–37364.

[21] Zhuang G, Wu X, Jiang Z, Kasman I, Yao J, Guan Y, Oeh J, Modrusan Z, Bais C, and Sampath D, et al (2012). Tumour-secreted miR-9 promotes endothelial cell migration and angiogenesis by activating the JAK-STAT pathway. *EMBO J* **31**, 3513–3523.

[22] Bordoli MR, Stiehl DP, Borsig L, Kristiansen G, Hausladen S, Schraml P, Wenger RH, and Camenisch G (2011). Prolyl-4-hydroxylase PHD2- and hypoxia-inducible factor 2-dependent regulation of amphiregulin contributes to breast tumorigenesis. *Oncogene* **30**, 548–560.

[23] Shoji M, Hancock WW, Abe K, Micko C, Casper KA, Baine RM, Wilcox JN, Danave I, Dillehay DL, and Matthews E, et al (1998). Activation of coagulation and angiogenesis in cancer: immunohistochemical localization in situ of clotting proteins and vascular endothelial growth factor in human cancer. *Am J Pathol* **152**, 399–411.

[24] Latasa MU, Salis F, Urtasun R, Garcia-Irigoyen O, Elizalde M, Uriarte I, Santamaria M, Feo F, Pascale RM, and Prieto J, et al (2012). Regulation of amphiregulin gene expression by beta-catenin signaling in human hepatocellular carcinoma cells: a novel crosstalk between FGF19 and the EGFR system. *PLoS One* **7**, e52711.

[25] Kim JH, Choi DS, Lee OH, Oh SH, Lippman SM, and Lee HY (2011). Antiangiogenic antitumor activities of IGFBP-3 are mediated by IGF-independent suppression of Erk1/2 activation and Egr-1-mediated transcriptional events. *Blood* **118**, 2622–2631.

[26] Liu B, Lee KW, Anzo M, Zhang B, Zi X, Tao Y, Shiry L, Pollak M, Lin S, and Cohen P (2007). Insulin-like growth factor-binding protein-3 inhibition of prostate cancer growth involves suppression of angiogenesis. *Oncogene* **26**, 1811–1819.

[27] Waugh DJ and Wilson C (2008). The interleukin-8 pathway in cancer. *Clin Cancer Res* **14**, 6735–6741.

[28] Jiang D, Guo H, Xu C, Chang J, Gu B, Wang L, Block TM, and Guo JT (2008). Identification of three interferon-inducible cellular enzymes that inhibit the replication of hepatitis C virus. *J Virol* **82**, 1665–1678.

[29] Degols G, Eldin P, and Mechti N (2007). ISG20, an actor of the innate immune response. *Biochimie* **89**, 831–835.

[30] Katsounas A, Rasimas JJ, Schlaak JF, Lempicki RA, Rosenstein DL, and Kottilil S (2014). Interferon stimulated exonuclease gene 20 kDa links psychiatric events to distinct hepatitis C virus responses in human immunodeficiency virus positive patients. *J Med Virol* **86**, 1323–1331.

[31] Wu X, Yang T, Liu X, Guo JN, Xie T, Ding Y, Lin M, and Yang H (2015). IL-17 promotes tumor angiogenesis through Stat3 pathway mediated upregulation of VEGF in gastric cancer. *Tumour Biol* **37**, 5439–5501.

[32] Liu Y, Luo F, Wang B, Li H, Xu Y, Liu X, Shi L, Lu X, Xu W, and Lu L, et al (2016). STAT3-regulated exosomal miR-21 promotes angiogenesis and is involved in neoplastic processes of transformed human bronchial epithelial cells. *Cancer Lett* **370**, 125–135.

[33] Dodd KM and Tee AR (2015). STAT3 and mTOR: co-operating to drive HIF and angiogenesis. *Oncoscience* **2**, 913–914.

[34] Cayrol F, Diaz Flaque MC, Fernando T, Yang SN, Sterle HA, Bolontrade M, Amoros M, Isse B, Farias RN, and Ahn H, et al (2015). Integrin alphavbeta3 acting as membrane receptor for thyroid hormones mediates angiogenesis in malignant T cells. *Blood* **125**, 841–851.

[35] Kress E, Skah S, Sirakov M, Nadjar J, Gadot N, Scoazec JY, Samarut J, and Plateroti M (2010). Cooperation between the thyroid hormone receptor TRalpha1 and the WNT pathway in the induction of intestinal tumorigenesis. *Gastroenterology* **138**, 1863–1874.

[36] Chung IH, Chen CY, Lin YH, Chi HC, Huang YH, Tai PJ, Liao CJ, Tsai CY, Lin SL, and Wu MH, et al (2015). Thyroid hormone-mediated regulation of

lipocalin 2 through the Met/FAK pathway in liver cancer. *Oncotarget* **6**, 15050–15064.

[37] Lin YH, Wu MH, Liao CJ, Huang YH, Chi HC, Wu SM, Chen CY, Tseng YH, Tsai CY, and Chung IH, et al (2015). Repression of microRNA-130b by thyroid hormone enhances cell motility. *J Hepatol* **62**, 1328–1340.